Multimagnon theory of antiferromagnetic resonance relaxation

S. M. Rezende*
Departamento de Fisica,† Universidade Federal de Pernambuco, Recife, Brazil
and Department of Physics, University of California, Santa Barbara, California 93106

R. M. White
Xerox Palo Alto Research Center, Palo Alto, California 94304
(Received 11 March 1976)

The temperature dependence of the linewidth of the antiferromagnetic resonance is shown to arise from multimagnon processes. At low temperatures a four-magnon process usually dominates. As the temperature increases towards the Néel temperature T_N, higher-order processes such as six-magnon, etc., become progressively more important. An analytic expression is derived for the n-magnon relaxation rate in the high-temperature limit. The theoretically predicted temperature and frequency dependence of the linewidth agrees quantitatively with data on MnF_2, FeF_2, $GdAlO_3$, Rb_2MnF_4, and K_2MnF_4 up to $0.8\,T_N$.

I. INTRODUCTION

The manner in which a magnetic system relaxes to equilibrium governs its device potential and also provides a test of both relevant microscopic interactions and theoretical methods. In many cases the device potential stimulates the need for microscopic understanding. For example, the tremendous potential in ferrite microwave devices led to a thorough investigation of the ferromagnetic resonance relaxation mechanism. Antiferromagnets have not had the benefit of such a driving technology. They do, however, share the same sublattice features as *canted* antiferromagnets such as the orthoferrites, or ferrimagnets, such as the garnets, near their compensation temperatures. Thus, antiferromagnets serve as prototypes for studying processes in multiple-sublattice systems in which the net magnetization is nearly zero.

The quantum theory of magnetic systems is complicated by the cyclic commutation relations of the components of the spin operators. Well below the magnetic ordering temperature it is possible to work in a boson representation which simplifies matrix elements and forms the basis for spin-wave theory. The only condition on the boson representation is that it satisfy the spin commutation relations. One such representation is that of Holstein and Primakoff[1] (HP)

$$\begin{aligned} S'_+ &= \sqrt{2S}\, a^\dagger (1 - a^\dagger a/2S)^{1/2}, \\ S'_- &= \sqrt{2S}\, (1 - a^\dagger a/2S)^{1/2}, \\ S'_z &= S - a^\dagger a . \end{aligned} \tag{1}$$

The boson operators $a^\dagger$ and a are associated with spin-wave, or magnon, creation and annihilation operators, respectively. The components of the spin $\vec{S}'$ defined by this transformation have the desired commutation relations. However, $\vec{S}'$ cannot be identified with the real spin $\vec{S}$, for the eigenvalues of S'_z, for example, have no lower bound whereas those of S_z do. Nevertheless, the matrix elements of an arbitrary function $G(\vec{S})$ of the components of the real spin $\vec{S}$ between the orthonormal eigenvectors of S_z, $|n\rangle$, may be related[2] to a matrix element of the HP spin $\vec{S}'$ in the larger Hilbert space spanned by the eigenvectors of $a^\dagger a$, Φ_n, according to

$$\langle n|\, G(\vec{S})\,|n'\rangle = (\Phi_n, G(P\vec{S}'P)\Phi_{n'}), \tag{2}$$

where P is the projection operator,

$$P\Phi_n = \begin{cases} \Phi_n, & n \leq 2S \\ 0, & n > 2S . \end{cases} \tag{3}$$

The spirit of spin-wave theory is to assume one is in a regime where $n \ll 2S$ so that the projection operator may be neglected.

Maleev[3] suggested an alternative representation based on Dyson's work,[4]

$$\begin{aligned} S''_+ &= \sqrt{2S}\, a^\dagger , \\ S''_- &= \sqrt{2S}\, [a - (1/2S)\, a^\dagger a a] , \\ S''_z &= S - a^\dagger a . \end{aligned} \tag{4}$$

We notice that the operators S''_+ and S''_- are not Hermitian in the Dyson-Maleev representation. As a result, one must introduce a metric operator F in order to define a scalar product. This has the property that

$$F_{n+1} = (1 - n/2S)\, F_n , \tag{5}$$

where

$$F_n = (\Phi_n, F\Phi_n) . \tag{6}$$

This metric operator also enters the relationship between the matrix elements of $\vec{S}$ and those of $\vec{S}''$,

$$\langle n|\, G(\vec{S})\,|n'\rangle = [1/(F_n F_{n'})^{1/2}](\Phi_n, FG(P\vec{S}''P)\Phi_{n'}) . \tag{7}$$

The presence of the metric operator F introduces the same nonlinearity that appears directly in the HP transformation.[5,6] This may easily be seen by taking $G(\vec{S}) = S_+$ in Eq. (7) and using Eq. (5). We shall see that these nonlinearities are responsible for the relaxation in antiferromagnets.

In principle there may be numerous boson representations each with its own metric. In this paper we shall use the HP approach.

The work presented here was motivated by the recent success in unraveling the intrinsic thermal contribution to the experimental antiferromagnetic-resonance (AFMR) linewidth. Due to the large AFMR frequency gap simple antiferromagnets such as MnF_2 and FeF_2 were initially studied with millimeter wavelength or far-infrared techniques. Despite the difficulties of working at these frequencies magnetic resonance studies of MnF_2,[7] and FeF_2,[8] were first carried out over fifteen years ago. Since then a number of theoretical attempts have been made to explain the observed linewidths. The mechanisms investigated include two-magnon pit scattering,[9] magnon-phonon scattering,[10] and four-magnon scattering.[11-17] Although some of these mechanisms gave a temperature dependence similar to that observed, the actual linewidths were orders of magnitude too small.

The key to this discrepancy was discovered by Kotthaus and Jaccarino[18] (KJ). By measuring the linewidth of MnF_2 in large magnetic fields and relatively low frequencies they found much smaller linewidths than those found at low fields and high frequencies. This indicated that the large linewidths observed in earlier experiments were largely due to radiation damping. Not only does radiation broadening contribute to the temperature-independent linewidth $\Delta H(0)$, but it also contributes a temperature dependence through the sublattice magnetization $M(T)$.

Once this contribution to the MnF_2 linewidth is eliminated,[19,20] one finds that the temperature-independent contribution is well explained by the two-magnon pit scattering calculated by Loudon and Pincus.[9] Similarly, the intrinsic temperature dependent contribution is well described up to a temperature of the order of $T_N/4$ by four-magnon scattering.[21] Above this temperature the linewidth increases more rapidly with temperature than four-magnon scattering predicts. The purpose of this paper is to show that this stronger temperature dependence may be described by higher-order magnon processes.[22] Such processes appear naturally in the Holstein-Primakoff representation through the expansion of the square root, and, as we shall show, are ubiquitous in antiferromagnets.

In Sec. II we derive the general expression for the relaxation of the AFMR due to its confluence with $\frac{1}{2}n-1$ thermal magnons to give $\frac{1}{2}n$ output magnons. The special case of $n=4$ is evaluated analytically within certain approximations, using the numerically evaluated results of White, Freedman, and Woolsey[21] (WFW) as a guide to the validity of these approximations. Using these approximations the temperature dependences of the higher-order processes are identified. In Sec. III these results are compared with data on several representative antiferromagnets, for which the intrinsic thermal contribution to ΔH has been extracted. These include MnF_2, FeF_2, $GdAlO_3$, and the two-dimensional antiferromagnets K_2MnF_4 and Rb_2MnF_4.

II. RELAXATION THEORY

A. Multimagnon Hamiltonian

We shall take for the Hamiltonian of our system that of a uniaxial two-sublattice antiferromagnet consisting of Zeeman, exchange, and anisotropy terms. The applied field is assumed to be parallel to the symmetry axis and smaller than the spin-flop critical field, so that

$$\mathcal{H} = g\mu_B H_0\left(\sum_i S_i^z + \sum_j S_j^z\right) + \sum_{ij} 2J_{ij}\vec{S}_i\cdot\vec{S}_j - K\left(\sum_i (S_i^z)^2 + \sum_j (S_j^z)^2\right), \tag{8}$$

where i and j refer to up and down spin sublattices, g is the electron gyromagnetic ratio, H_0 is the applied magnetic field, J_{ij} is the exchange constant, and K is the phenomenological anisotropy constant. The anisotropy energy has different origins in different materials. When these differences are taken into account the form of the anisotropy energy in Eq. (8) may vary. One result of this is to make the anisotropy contribution to the spin-wave energy wave-vector dependent. Although this may affect certain thermodynamic properties of the system it will not affect the results of this paper where the exchange interaction is always the dominant interaction. In the crystals we shall consider the exchange interaction is strongest between spins on opposite sublattices (which are second nearest neighbors in MnF_2 and FeF_2). Therefore, for the sake of simplicity we write the exchange term as

$$2J_2\sum_{i,\,j=i+\delta}\vec{S}_i\cdot\vec{S}_j = J_2\sum_{i,j}(2S_i^zS_j^z + S_i^+S_j^- + S_i^-S_j^+) . \tag{9}$$

A HP boson representation is introduced for both sublattices,

$$S_i^+ = \sqrt{2S}\, f_i\, a_i, \quad S_j^+ = \sqrt{2S}\, b_j^\dagger f_j,$$
$$S_i^- = \sqrt{2S}\, a_i^\dagger f_i, \quad S_j^- = \sqrt{2S}\, f_j\, b_j, \tag{10}$$
$$S_i^z = S - a_i^\dagger a_i, \quad S_j = -S + b_j^\dagger b_j,$$

where

$$f_i = (1 - a_i^\dagger a_i/2S)^{1/2}, \quad f_j = (1 - b_j^\dagger b_j/2S)^{1/2}. \tag{11}$$

As long as one is not very close to the Néel temperature, the square roots in Eq. (11) can be expanded in a power series which takes the form

$$f_i = 1 - \sum_{n=1}^{\infty} \frac{(2n-3)!!}{2^n n!} \left(\frac{a_i^\dagger a_i}{2S}\right)^n, \tag{12}$$

where $(2n-3)!! = 1\times3\times5\times\cdots\times(2n-3)$.

In the usual manner one defines spatial Fourier transforms of the boson operators

$$a_i = N^{-1/2} \sum_{\vec{k}} a_{\vec{k}} e^{i\vec{k}\cdot\vec{r}_i}, \quad b_j = N^{-1/2} \sum_{\vec{k}} b_{\vec{k}} e^{i\vec{k}\cdot\vec{r}_j}, \tag{13}$$

where N is the number of spins per sublattice in the crystal. In terms of these operators the Hamiltonian, Eq. (8), takes the form

$$\mathcal{H} = E_0 + \mathcal{H}^{(2)} + \mathcal{H}^{(4)} + \mathcal{H}^{(6)} + \cdots, \tag{14}$$

where each term contains an even number of boson operators including various intra- and intersublattice couplings. In order to diagonalize the quadratic part of the Hamiltonian one introduces new boson operators by a Bogoliubov transformation[23]

$$a_{\vec{k}} = u_{\vec{k}}\alpha_{\vec{k}} - v_{\vec{k}}\beta_{-\vec{k}}^\dagger, \quad b_{-\vec{k}}^\dagger = -v_{\vec{k}}\alpha_{\vec{k}} + u_{\vec{k}}\beta_{-\vec{k}}^\dagger. \tag{15}$$

In Eq. (15) $\alpha_{\vec{k}}$ and $\beta_{\vec{k}}$ are the new normal mode boson operators associated with eigenvalues one of which decreases with increasing applied field and the other of which increases with the field.

The transformation coefficients are given by

$$u_{\vec{k}} = [(A + \omega_{\vec{k}})/2\omega_{\vec{k}}]^{1/2}, \quad v_{\vec{k}} = (u_{\vec{k}}^2 - 1)^{1/2}, \tag{16}$$

with

$$A = \gamma(H_E + H_A), \tag{17}$$

$$\omega_{\vec{k}} = \gamma[(2H_E + H_A)H_A + H_E^2(1 - \gamma_{\vec{k}}^2)]^{1/2}$$
$$= \gamma[H_c^2 + H_E^2(1 - \gamma_k^2)]^{1/2}, \tag{18}$$

$$\gamma_{\vec{k}} = \frac{1}{z_2} \sum_{i=1}^{z_2} e^{i\vec{k}\cdot\vec{\delta}_i}, \tag{19}$$

$$H_E = 2Sz_2J_2/\gamma\hbar, \quad H_A = (2S-1)K/\gamma\hbar, \tag{20}$$

where z_2 is the number of intersublattice nearest neighbors. For a body-centered tetragonal lattice $\gamma_{\vec{k}}$ becomes

$$\gamma_{\vec{k}} = \cos\tfrac{1}{2}k_x a \cos\tfrac{1}{2}k_y a \cos\tfrac{1}{2}k_z c. \tag{21}$$

Note that $\gamma_0 = 1$ while $\gamma_{k_{ZB}} = 0$. The quadratic part of the Hamiltonian then becomes

$$\mathcal{H}^{(2)} = \sum_{\vec{k}} (\hbar\omega_{\alpha\vec{k}}\alpha_{\vec{k}}^\dagger\alpha_{\vec{k}} + \hbar\omega_{\beta\vec{k}}\beta_{\vec{k}}^\dagger\beta_{\vec{k}}), \tag{22}$$

where

$$\omega_{\alpha\vec{k}} = \omega_{\vec{k}} - \gamma H_0, \quad \omega_{\beta\vec{k}} = \omega_{\vec{k}} + \gamma H_0. \tag{23}$$

The higher-order terms of the Hamiltonian, Eq. (14), must also be transformed according to Eq. (15). When this is done we obtain terms which contain all types of combinations of $\alpha_{\vec{k}}$, $\alpha_{\vec{k}}^\dagger$, $\beta_{\vec{k}}$, and $\beta_{\vec{k}}^\dagger$ operators. The paper of Harris, Kumar, Halperin, and Hohenberg[17] (HKHH) contains the detailed form of $\mathcal{H}^{(4)}$. As shown by those authors and in WFW, the only four-magnon processes which contribute to the relaxation of antiferromagnetic magnons are those described by terms of the type $\alpha_{k1}^\dagger\alpha_{k2}^\dagger\alpha_{k3}\alpha_{k4}$, $\alpha_{k1}^\dagger\beta_{k2}^\dagger\alpha_{k3}\beta_{k4}$, and $\beta_{k1}^\dagger\beta_{k2}^\dagger\beta_{k3}\beta_{k4}$. The diagrams for these processes that can relax a $k = 0$ α mode are shown in Fig. 1(a). Using energy-momentum conservation arguments one can extend the results of four-magnon processes to general n-magnon (n even) processes and conclude that the major contributions to the decay rate involve the absorption and emission of $\frac{1}{2}n$ magnons. These may all involve the same mode (intramode scattering) or may involve intermode scattering. The n-magnon term is illustrated in Fig. 1(b). The n-magnon Hamiltonian for intramode scattering can be expressed in the following form:

$$\mathcal{H}^{(n)} = \sum_{\vec{k}_1\vec{k}_2\cdots\vec{k}_n} C^{(n)}_{\vec{k}_1\vec{k}_2\cdots\vec{k}_n} \alpha_{\vec{k}_1}^\dagger \alpha_{\vec{k}_2}^\dagger \cdots \alpha_{\vec{k}_{n/2}}^\dagger \alpha_{\vec{k}_{n/2+1}} \cdots \alpha_{\vec{k}_n}$$
$$\times \Delta(\vec{k}_1 + \vec{k}_2 + \cdots \vec{k}_{n/2} - \cdots - \vec{k}_n). \tag{24}$$

B. Relaxation rate

The expression for the relaxation rate of a given k_1 mode can be derived in a manner similar to that employed for three-magnon processes based on the Fermi golden rule.[24] This gives the same result that one obtains by calculating the imaginary part of the magnon self-energy to lowest order. Denoting by n_1 the occupation number of the k_1 mode, the relaxation rate η_1 is defined by

$$\frac{dn_1}{dt} = -\eta_1(n_1 - \bar{n}_1), \tag{25}$$

where $\bar{n}_1$ represents the thermal equilibrium occupancy. η_1 is the total relaxation rate obtained by summing over the relaxation rates $\eta_1^{(n)}$ associated with the different n-magnon channels. With Eqs. (24) and (25), and the use of the golden rule, one can show that

$$\eta_1^{(n)} = \frac{2\pi}{\hbar^2}(1 - e^{-\beta\hbar\omega_1}) \times \sum_{\vec{k}_2\vec{k}_3\cdots\vec{k}_n} |C^{(n)}|^2 \bar{n}_2\bar{n}_3\cdots\bar{n}_{n/2}(\bar{n}_{n/2+1}+1)\cdots \times(\bar{n}_n+1)\delta(\omega)\Delta(\vec{k}), \quad (26)$$

where

$$\beta = 1/k_B T,$$
$$\bar{n}_k = (e^{\beta\hbar\omega_k} - 1)^{-1},$$
$$\delta(\omega) = \delta(\omega_1+\omega_2+\cdots+\omega_{n/2}-\omega_{n/2+1}-\cdots-\omega_n),$$
$$\Delta(\vec{k}) = \Delta(\vec{k}_1+\vec{k}_2+\cdots+\vec{k}_{n/2}-\vec{k}_{n/2+1}-\cdots-\vec{k}_n).$$

Using energy conservation and the result $(\bar{n}_k+1)/\bar{n}_k = e^{\beta\hbar\omega_k}$ we can write an alternative expression for Eq. (26) which we shall prefer to use in this paper,

$$\eta_1^{(n)} = \frac{2\pi}{\hbar^2}(e^{\beta\hbar\omega_1} - 1) \times \sum_{\vec{k}_2\vec{k}_3\cdots\vec{k}_n} |C^{(n)}|^2 e^{\beta\hbar(\omega_2+\omega_3+\cdots+\omega_{n/2})} \times \bar{n}_2\bar{n}_3\cdots\bar{n}_n\delta(\omega)\Delta(\vec{k}) \quad (27)$$

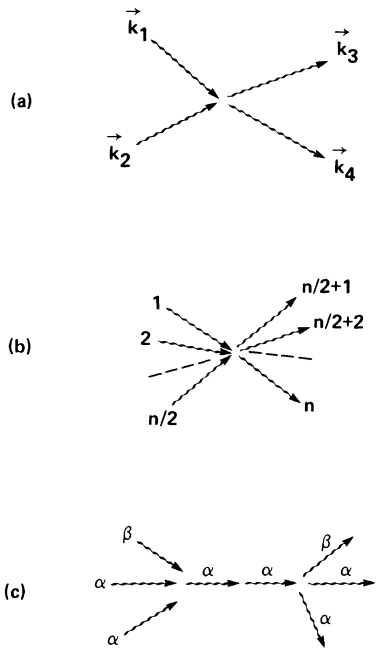

FIG. 1. Various multimagnon processes: (a) four-magnon process; (b) n-magnon process, as the term is used in this paper; (c) six-magnon process arising from the four-magnon process carried to second order in perturbation theory.

C. Four-magnon relaxation

For $n = 4$ Eq. (27) was evaluated numerically by WFW for MnF_2. The sums over the six coordinates associated with the two independent wave vectors were evaluated by dividing the range from $k = 0$ to the Brillouin zone boundary (k_{ZB}) into 50 points and weighting the contribution of each point to the sum appropriately. This process involved 50^6 operations, which took about 90 min to run on a fast computer. Similar numerical computations of high-order processes would become prohibitively long. The analytic evaluation of Eq. (27) for large values of n, on the other hand, becomes very difficult, and has to be done under suitable approximations. A similar problem was faced by Sparks and Sham[25] in dealing with multiphonon absorption. However, in their case they had one virtual phonon of frequency ω decaying into n phonons. These n phonons were all assumed to have the same frequency ω_g, the frequency at which the density of states is largest. In our case the situation is more complicated because we have additional input particles whose frequencies depend upon the temperature, as does the density of states. Our first step, therefore, is to develop approximations for the four-magnon process which lead to reasonably simple calculations. The results are tested against the accurate results of WFW and the experimental data for MnF_2. Once the various approximations are understood they may then be applied to higher-order processes. The approximations developed are such that one can obtain completely analytical results in some cases, such as for MnF_2 in the high-temperature regime. In other cases the approximations yield expressions which can be evaluated by reasonable numerical integrations in k space. This section will be devoted to the presentation of the model developed for the calculation of four-magnon scattering relaxation rate.

Four-magnon terms arise from both the exchange and the anisotropy energies in Eq. (8). The processes that can relax a $k = 0$ α mode can be of the "intramode" type, in which only α modes are involved, or of the "intermode" type. The Hamiltonian for the former is

$$\mathcal{H}^{\alpha-\alpha} = \sum_{\substack{\vec{k}_1,\vec{k}_2\\ \vec{k}_3,\vec{k}_4}} C^{\alpha-\alpha}_{\vec{k}_1\vec{k}_2\vec{k}_3\vec{k}_4} \alpha^\dagger_{\vec{k}_1}\alpha^\dagger_{\vec{k}_2}\alpha_{\vec{k}_3}\alpha_{\vec{k}_4}\Delta(\vec{k}_1+\vec{k}_2-\vec{k}_3-\vec{k}_4), \quad (28)$$

where

$$C^{\alpha-\alpha}_{\vec{k}_1\vec{k}_2\vec{k}_3\vec{k}_4} = (J_2 z_2/2N)\,(u_{\vec{k}_1} v_{\vec{k}_2} v_{\vec{k}_3} v_{\vec{k}_4}\gamma_{\vec{k}_1} + u_{\vec{k}_1} u_{\vec{k}_2} u_{\vec{k}_3} v_{\vec{k}_4}\gamma_{\vec{k}_4} + u_{\vec{k}_1} v_{\vec{k}_2} u_{\vec{k}_3} u_{\vec{k}_4}\gamma_{\vec{k}_2} + v_{\vec{k}_1} v_{\vec{k}_2} u_{\vec{k}_3} v_{\vec{k}_4}\gamma_{\vec{k}_3}$$
$$- 4u_{\vec{k}_1} v_{\vec{k}_2} u_{\vec{k}_3} v_{\vec{k}_4}\gamma_{\vec{k}_2-\vec{k}_4}) - (K/N)\,(u_{\vec{k}_1} u_{\vec{k}_2} u_{\vec{k}_3} u_{\vec{k}_4} + v_{\vec{k}_1} v_{\vec{k}_2} v_{\vec{k}_3} v_{\vec{k}_4})\,. \tag{29}$$

The Hamiltonian for the absorption of an α- and a β-mode magnon and emission of new α and β magnons is

$$\mathcal{H}^{\alpha-\beta}_{ex} = \sum_{\substack{\vec{k}_1,\vec{k}_2\\ \vec{k}_3,\vec{k}_4}} C^{\alpha-\beta}_{\vec{k}_1\vec{k}_2\vec{k}_3\vec{k}_4}\,\alpha^{\dagger}_{\vec{k}_1}\beta^{\dagger}_{\vec{k}_2}\alpha_{\vec{k}_3}\beta_{\vec{k}_4}\Delta(\vec{k}_1+\vec{k}_2-\vec{k}_3-\vec{k}_4)\,, \tag{30}$$

where

$$C^{\alpha-\beta}_{\vec{k}_1\vec{k}_2\vec{k}_3\vec{k}_4}$$
$$= (J_2 z_2/N)\,(u_{\vec{k}_1} u_{\vec{k}_2} u_{\vec{k}_3} v_{\vec{k}_4}\gamma_{\vec{k}_2} + u_{\vec{k}_1} v_{\vec{k}_2} v_{\vec{k}_3} v_{\vec{k}_4}\gamma_{\vec{k}_3} + u_{\vec{k}_1} u_{\vec{k}_2} v_{\vec{k}_3} u_{\vec{k}_4}\gamma_{\vec{k}_1} + v_{\vec{k}_1} u_{\vec{k}_2} v_{\vec{k}_3} v_{\vec{k}_4}\gamma_{\vec{k}_4} + v_{\vec{k}_1} v_{\vec{k}_2} v_{\vec{k}_3} u_{\vec{k}_4}\gamma_{\vec{k}_2}$$
$$+ v_{\vec{k}_1} u_{\vec{k}_2} u_{\vec{k}_3} u_{\vec{k}_4}\gamma_{\vec{k}_3} + v_{\vec{k}_1} v_{\vec{k}_2} u_{\vec{k}_3} v_{\vec{k}_4}\gamma_{\vec{k}_1} + u_{\vec{k}_1} v_{\vec{k}_2} u_{\vec{k}_3} u_{\vec{k}_4}\gamma_{\vec{k}_4} - 2u_{\vec{k}_1} u_{\vec{k}_2} u_{\vec{k}_3} u_{\vec{k}_4}\gamma_{\vec{k}_2-\vec{k}_4} - 2u_{\vec{k}_1} v_{\vec{k}_2} v_{\vec{k}_3} u_{\vec{k}_4}\gamma_{\vec{k}_3-\vec{k}_4}$$
$$- 2v_{\vec{k}_1} u_{\vec{k}_2} u_{\vec{k}_3} v_{\vec{k}_4}\gamma_{\vec{k}_2+\vec{k}_1} - 2v_{\vec{k}_1} v_{\vec{k}_2} v_{\vec{k}_3} v_{\vec{k}_4}\gamma_{\vec{k}_3-\vec{k}_1}) - 4(K/N)\,(u_{\vec{k}_1} v_{\vec{k}_2} u_{\vec{k}_3} v_{\vec{k}_4} + v_{\vec{k}_1} u_{\vec{k}_2} v_{\vec{k}_3} u_{\vec{k}_4})\,. \tag{31}$$

The following approximations were employed in evaluating $\eta_1^{(4)}$.

(a) The sums in Eq. (27) were converted into integrals in k space according to the usual relation

$$\sum_{\vec{k}} \rightarrow \frac{N\Omega}{(2\pi)^3}\int k^2\,dk\,d(\cos\theta)\,d\phi\,. \tag{32}$$

(b) The magnon dispersion relation was approximated by $\omega_k = \omega_0 + \bar{v}k$, where $\bar{v}$ expresses an average magnon velocity. As will be discussed later in the applications of the theory, magnon renormalization is introduced in ω_k through $\bar{v}(T)$. The use of the linear dispersion relation is justified for MnF_2 by the fact that in the temperature range where magnon-magnon interactions dominate the relaxation, which is approximately $0.1T_N < T < 0.8T_N$, magnons from the whole Brillouin zone contribute to the decay of the $k = 0$ mode. This is illustrated by Fig. 2, which shows plots of the weighted α mode population for MnF_2 in the presence of a magnetic field close to the spin-flop value for several temperatures, using the exact dispersion relation. Since a linear function is the best simple relation that describes the magnon frequencies over the whole zone, it was chosen to represent ω_k. It should be pointed out, however, that the use of a linear dispersion relation is not essential for a simple numerical evaluation of the four-magnon relaxation rate. In fact we have also done calculations with the nearly exact spherical model $\omega_k = \gamma(H_c^2 + H_E^2 \sin^2\tilde{k})^{1/2} \pm \gamma H_0$, where $\tilde{k} = \frac{1}{2}k\tilde{a}$, $\tilde{a}$ being an effective lattice parameter to be adjusted for different cases. However, as will be seen below, the linear approximation greatly simplifies the energy-momentum conservation rules in such a manner that the calculations can be extended to higher-order processes.

The linear approximation to the dispersion relation enables us to simplify the energy-conserving δ function considerably. Since the uniform precession mode has no momentum, i.e., $\vec{k}_1 = 0$, then $\vec{k}_4 = \vec{k}_2 - \vec{k}_3$. Using this expression and the linear dispersion relation in the energy δ function gives

$$\delta(\omega_1 + \omega_2 - \omega_3 - \omega_4) = \delta(\bar{v}k_2 - \bar{v}k_3 - \bar{v}\,|\,\vec{k}_2 - \vec{k}_3\,|)$$
$$= [(k_2 - k_3)/\bar{v}k_2k_3]\,\delta(\cos\theta_{23} - 1),$$
$$k_2 \geq k_3 \tag{33}$$

where θ_{23} is the angle between $\vec{k}_2$ and $\vec{k}_3$ and the

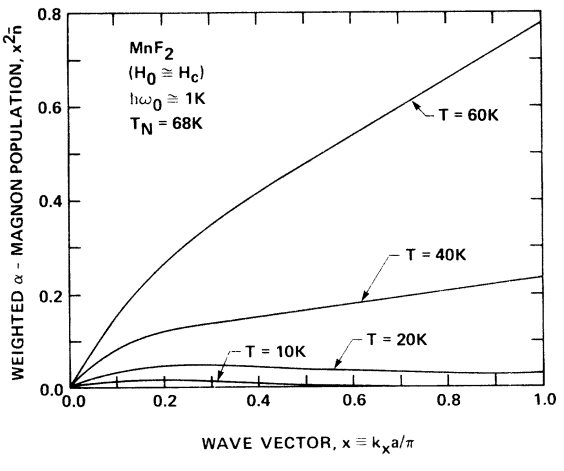

FIG. 2. Weighted magnon population curves as a function of wave vector for MnF_2 in the presence of an applied field equal to that employed in the linewidth measurements discussed in this paper (Ref. 18).

condition $k_2 \geq k_3$ also follows from energy conservation. The integral over $\vec{k}_4$ has been eliminated by the Kronecker delta $\Delta(\vec{k})$. The integrals in θ_2, ϕ_2, and ϕ_3 are freely evaluated, giving $8\pi^2$. The integral over θ_3 is taken care of by the δ function, Eq. (33). With approximations (a) and (b), the four-magnon decay rate for the $k_1 = 0$ mode obtained from Eq. (27) becomes

$$\eta_1^{(4m)} = \frac{2\Omega^2(e^{\beta\hbar\omega_1}-1)}{\hbar^2 \bar{v}(2\pi)^3} \int_0^{k_{\max}} dk_2 k_2 \frac{e^{\beta\hbar\omega_2}}{e^{\beta\hbar\omega_2}-1} \int_0^{k_2} dk_3 k_3(k_2-k_3) \frac{(NC)^2}{(e^{\beta\hbar\omega_3}-1)(e^{\beta\hbar\omega_{2-3}}-1)}, \tag{34}$$

where $k_{\max}$ will be defined below Eq. (44).

To calculate the α-intramode decay rate from Eq. (34) we use $\omega_k = \omega_0 + \bar{v}k$ in all magnon frequency modes and take

$$[C^{(4)}]^2 = \tfrac{1}{2}[C^{\alpha\alpha}_{1234} + C^{\alpha\alpha}_{2134} + C^{\alpha\alpha}_{1243} + C^{\alpha\alpha}_{2143}]^2, \tag{35}$$

where the factor of $\frac{1}{2}$ accounts for the fact that the two output magnons are equivalent, and that the processes in which they are exchanged should not be counted twice.

Since $\omega_0 = \gamma(H_c - H_0)$, the frequency of a β mode is taken to be $\omega_{\beta k} = \omega_{\alpha k} - 2\omega_0 + 2\gamma H_c$. Therefore, the intermode scattering contribution for the decay of a $k = 0$ α mode is obtained from Eq. (34) by using $\omega_{\beta k}$ for ω_2 and ω_4, $\omega_{\alpha k}$ for ω_3, and $[C^{(4)}]^2 = (C^{\alpha\beta}_{1234})^2$.

Equation (34) is already in a form which lends itself to reasonably simple numerical calculations. These will be discussed in Sec. III.

At this point let us introduce an additional approximation to obtain a full analytical evaluation of the four-magnon relaxation rate, valid for MnF_2 in the high-field case.

(c) Since with $k_1 = 0$, the energy-momentum conservation requires that k_2, k_3, and k_4 be collinear [Eq. (33)]. For temperatures above about $0.1T_N$, the joint density of states is largest when $k_2 \simeq k_3 \simeq k$(large) and $k_4 \approx 0$ in one of the possible scattering processes. Thus the vertex for this process can be approximated by $C^{(4)}_{0kk0}$. Also numerical investigations show that $C^{(4)}_{0kk0}$ is nearly independent of k. Therefore, we approximate the coupling coefficients for the four-magnon processes by

$$C^{(4)}_{\alpha\alpha} = C^{(4)}_{0k_{ZB}k_{ZB}0} + C^{(4)}_{k_{ZB}0k_{ZB}0} + C^{(4)}_{0k_{ZB}0k_{ZB}} + C^{(4)}_{k_{ZB}00k_{ZB}}, \tag{36}$$

$$C^{(4)}_{\alpha\beta} = C^{(4)}_{0k_{ZB}0k_{ZB}}. \tag{37}$$

This greatly simplifies the expression for the coupling coefficient due to the fact that at the zone boundary $\gamma_{ZB} = v_{ZB} = 0$, $u_{ZB} = 1$, and at the center of the Brillouin zone $\gamma_0 = 1$. With Eqs. (29), (31), (36), and (37) we have

$$NC^{\alpha\alpha} = (u_0 v_0 - v_0^2)\, 2z_2 J_2 - 4u_0^2 K, \tag{38}$$

$$NC^{\alpha\beta} = -(2u_0^2 - u_0 v_0) z_2 J_2 - 4v_0^2 K. \tag{39}$$

Note that since $u_0 > v_0$ (for MnF_2 $u_0 = 1.87$ and $v_0 = 1.58$), the exchange and anisotropy scattering amplitudes interfere destructively in the intramode case, Eq. (38), whereas in the intermode case, Eq. (39), they interfere constructively.

With Eqs. (38) and (39) the coupling coefficients can be taken out of the integrals in Eq. (34). The temperature dependence of the relaxation is now entirely contained in the exponential functions. This dependence can be studied in two limiting approximations: a low-temperature approximation, which is valid in the range where most of the contribution to the integrals comes from the region in k space where $\hbar\omega_k \gg k_B T$; and a high-temperature limit in which $\hbar\omega_k \ll k_B T$. We further assume that $\hbar\omega_0 \ll k_B T$, which is satisfied in the high-field experiments on MnF_2. We now write Eq. (34) as

$$\eta_1^{(4m)} = [2\Omega^2\omega_0/(2\pi)^3]\,(NC)^2\,[(k_B T)^4/(\hbar\bar{v})^6]\, I^{(4)}(T), \tag{40}$$

where

$$I^{(4)}(T) = \int_0^{x_{\max}} dx \int_0^x dy \frac{xe^x}{e^x - 1} \frac{y}{e^y - 1} \frac{x-y}{e^{x-y}-1} \tag{41}$$

and

$$x = \hbar\bar{v}k_2/k_B T, \quad y = \hbar\bar{v}k_3/k_B T. \tag{42}$$

In the low-temperature regime the integral peaks at a value of $x \ll x_{\max}$, and therefore the upper limit of the integral in x can be extended to infinity. In Fig. 2 we can see that this is a good approximation in MnF_2 at temperatures below about 20 °K, which is approximately $\frac{1}{4}T_N$. In this regime the three exponentials are all much larger than unity so that Eq. (41) becomes

$$I^{(4)}(T)\big|_{\text{low}\,T} = \int_0^\infty dx\, xe^x \int_0^x dy\, y(x-y) = 4. \tag{43}$$

Since this integral is independent of the temperature, in the low-temperature region the four-magnon relaxation rate is proportional to T^4.

As the temperature increases higher-energy magnon states become more populated and the peak of the integrand in Eq. (41) shifts towards

the Brillouin zone boundary. This is clearly seen in Fig. 2. As a consequence the upper limit of the integral in x limits the increase of the net magnon population with increasing temperature. Since $x_{\max} \propto 1/T$, the temperature dependence of the relaxation rate is smaller than at lower temperatures. In order to evaluate Eq. (41) in this regime we further assume that $\hbar\omega_k \ll k_B T$ and make a binomial expansion of all exponentials. Keeping only the lowest-order terms, $I^{(4)}$ reduces to

$$I^{(4)}(T)\big|_{\text{high}T} = \int_0^{x_{\max}} dx \int_0^x dy = \tfrac{1}{2} x_{\max}^2 . \tag{44}$$

We can now compare the analytical results, Eqs. (40)–(44), with the experimental data of Kotthaus and Jaccarino for MnF_2 and with the numerical calculation of WFW. We take $\omega_0 = 1.4\times10^{11}$ sec^{-1}, $u_0 = 1.82$, $v_0 = 1.52$, $J_2 = 1.84$ °K, $z_2 = 8$, $2K = 0.52$ °K (these values correspond to $H_E = 549$ kOe and $H_A = 7.87$ kOe), and $\Omega = (4.87)^2(3.3)$ Å^3. For $k_{\max}$ we use the value $\pi/\Omega^{1/3}$. This does not correspond to the value of $k_{\max}$ which yields a total number of magnon modes in the spherical zone equal to N. We shall return to this point later. At low temperatures we use $\bar{v} = [\omega(k_{\max}) - \omega_0]/k_{\max} \simeq 1.2 \times10^5$ cm/sec and at high temperatures we take $\bar{v} = 1.1\times10^5$ cm/sec to account for the renormalization of the magnon energy. In the two limiting situations the intramode four-magnon relaxation rate becomes

$$\eta_1^{(4m)} = \begin{cases} 2.2\times10^3 T^4 \text{ sec}^{-1}, & T < \tfrac{1}{4}T_N \\ 2.06\times10^6 T^2 \text{ sec}^{-1}, & T > \tfrac{1}{4}T_N . \end{cases} \tag{45}$$

This result is shown as dashed lines in Fig. 3. In the two temperature limits these analytic results overestimate the relaxation rate slightly. For $T < \frac{1}{4}T_N$ both the analytic result and the WFW calculation give a T^4 dependence for the linewidth and are in good agreement with the KJ data for MnF_2. Above $\frac{1}{4}T_N$ the experimental data maintain its T^4 dependence, but the four-magnon decay rate assumes a T^2 dependence, for the reason explained above. This suggested to us, that other interaction processes come into play and dominate the relaxation rate of the $k = 0$ magnon mode in this high-temperature regime. Below we shall, in fact, show that higher-order magnon processes give such a behavior.

At this point it is worth comparing our results with those of other authors. First of all we note that four-magnon processes have been considered as the prevailing mechanism for the thermal decay of magnons in antiferromagnets, but there is considerable disagreement concerning the explicit temperature dependence of the linewidth. Except for the recent work of WFW, none of the previous treatments have given the observed T^4 dependence. The most complete treatment of the problem is that of HKHH.[17] They have treated only the case of zero applied field, but their regime B', which corresponds to $\gamma\hbar H_c \ll k_B T \ll k_B T_N$, is essentially our small ω_0, low-temperature regime. In this situation they obtain a temperature dependence of the form $T^3 \ln(k_B T/\hbar\omega_0)$ which does not agree with our results. Since the vertices for the four-magnon process in the Dyson-Maleev and in the Holstein-Primakoff formalisms are the same and the relaxation rate equation used by HKHH is the same as ours, the origins of the discrepancy between the two results lie only on the different approximations used in the evaluation of the integrals. These are mainly the form of the dispersion relation and the approximations made in the coupling coefficients. At higher temperatures the calculation of HKHH fails because they maintain the upper limit of the last integral in k as infinity.

D. Higher-order magnon relaxation

Let us now use the experience gained in Sec. II C to evaluate the general n-magnon process given by Eq. (27). In particular, let us employ the same approximations:

(a) The sums over wave vectors are replaced by integrals according to

$$\sum_{\vec{k}_m} \to \int \frac{N\Omega}{(2\pi)^3} k_m^2 \, dk_m \, d(\cos\theta_m) \, d\phi_m . \tag{46}$$

Since momentum conservation removes one of the

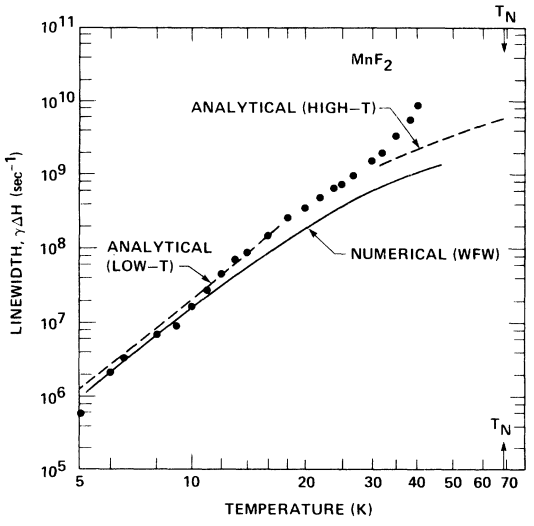

FIG. 3. Comparison of the high- and low-temperature approximations of the four-magnon process with the numerical evaluation of White *et al.* (Ref. 21). The points are the experimental data of Kotthaus and Jaccarino (Ref. 18).

integrals in $\vec{k}$ space and $\vec{k}_1 = 0$, there are $n-2$ integrals over k_m, θ_m, and ϕ_m.

(b) The dispersion relation is assumed linear. Even with this approximation the manner in which energy and momentum are conserved becomes complicated.

In order to simplify matters we shall make an additional approximation (b′) that all the wave vectors are collinear. The energy δ function then becomes

$$\delta(\omega) = \frac{\hbar}{k_B T} \frac{|x - x_{n-1}|}{x x_{n-1}} \delta(\cos\theta_{n-1} - 1), \tag{47}$$

where $x = x_2 + x_3 + \cdots + x_{n/2} - x_{n/2+1} - \cdots - x_{n-2}$,

$x_n = \hbar \bar{v} k_n / k_B T$

and θ_{n-1} is the angle between $\vec{k}_{n-1}$ and $\vec{k} = \vec{k}_2 + \cdots - \vec{k}_{n-2}$. As a result of this restriction on θ_{n-1} there remain $n-3$ integrations over θ_m and $n-2$ over ϕ_n.

(c) If we now approximate the coupling coefficient $C^{(n)}$ by an average value $\bar{C}^{(n)}$ the relaxation rate becomes

$$\eta_1^{(n)} = \alpha^{(n)} I^{(n)}(T)\, T^{3n-8}, \tag{48}$$

where

$$\alpha^{(n)} = \pi \omega_0 |\bar{C}^{(n)}|^2 \left(\frac{N\Omega}{2\pi^2}\right)^{n-2} \frac{k_B^{3n-8}}{(\hbar \bar{v})^{3n-6}} \tag{49}$$

and

$$I^{(n)}(T) = \int_0^{x_{\max}} x_2^2 dx_2 \cdots \int_0^{x_{\max}} x_{n/2}^2 dx_{n/2} \int_0^{(x_2 + x_3 \cdots x_{n/2})'} x_{n/2+1}^2 dx_{n/2+1} \cdots \times \int_0^{x'} x_{n-1}^2 dx_{n-1} e^{(x_2 + x_3 + \cdots x_{n/2})} \bar{n}_2 \bar{n}_3 \cdots \bar{n}_n \frac{|x - x_{n-1}|}{x x_{n-1}}. \tag{50}$$

Note that energy and momentum conservation set the upper limits of the integrals associated with the output magnons and makes $\bar{n}_n = (e^{(x - x_{n-1})} - 1)^{-1}$. The primes have the meaning,

$$x' = \begin{cases} x, & x < x_{\max} \\ x_{\max}, & x \geq x_{\max}, \end{cases} \tag{51}$$

where $x_{\max} = \hbar k_{\max} \bar{v} / k_B T$.
It is through these limits that $I^{(n)}(T)$ acquires its temperature dependence.

1. Low-temperature limit

In the low-temperature limit the exponentials in the integrand ensure that integral is insensitive to the upper limit making $I^{(n)}(T)$ independent of temperature. Therefore

$$\eta_1^{(n)}|_{\text{low}T} \sim T^{3n-8}. \tag{52}$$

2. High-temperature limit

In the high-temperature limit the magnon distribution peaks at the Brillouin-zone boundary. Thus the thermal input magnons may all be taken to have $k \approx k_{ZB}$. Similarily $\frac{1}{2}n - 1$ of the output magnons will have zone-boundary wave vectors and one with $k \approx 0$. In this case the upper limits of $I^{(n)}(T)$ in Eq. (50) will become $x_{\max}$. The integrations thus "decouple" giving $I^{(n)}(T) \sim (\frac{1}{2} x_{\max}^2)^{n-3}$. Since $x_{\max} \sim 1/T$ the high-temperature dependence of the relaxation rate is

$$\eta_1^{(n)}|_{\text{high}T} \sim T^{n-2}. \tag{53}$$

Due to the fact that all the magnons but two have $k \sim k_{ZB}$ only terms with one v_k exist in the effective vertex for the n-magnon interaction. These arise from the expansions of S^+ and S^- in Eq. (9), in which only the two terms with $(n-1)$ a_i operators and one b_j operator are retained. From Eqs. (9)–(12) it is not difficult to show that the terms involving only α modes have the form

$$C_{12\cdots n}^{(n)} = \frac{2 J_2 z_2}{2^{n-2} N^{n/2-1} S^{n/2-2}} \frac{(n-5)!!}{(\frac{1}{2}n - 1)!} \times (v_1 u_2 u_3 \cdots u_n \gamma_1 + u_1 u_2 \cdots u_{n-1} v_n \gamma_n). \tag{54}$$

As we have seen above this gives the dominant contribution to the relaxation rate. Therefore, we shall neglect the α-β combinations.

To find the effective coupling constant we set all $k = k_{ZB}$ except two, which are made equal to zero, one of them being the one for the v_n. The sum of all nonzero terms will give a factor of $(\frac{1}{2}n)!\,(\frac{1}{2}n - 1)!$. As there are also $(\frac{1}{2}n)!\,(\frac{1}{2}n - 1)!$ identical magnons, the factor entering the effective vertex is the square root of this number. The effective vertex then becomes

$$\overline{C}^{(n)} = b_{(n)} \frac{u_0 v_0 J_2 z_2}{S^{n/2-2} N^{n/2-1}} , \tag{55}$$

where

$$b_{(n)} = \sqrt{\tfrac{1}{2}n}\,(n-5)!!/2^{n-4} . \tag{56}$$

There are also contributions to the n-magnon vertex arising from combinations of lower-order processes. In Fig. 1(c), for example, we indicate how one of the four-magnon processes in second order leads to an effective six-magnon process. The effective interaction associated with this process is

$$\mathcal{H}^{(6)} = \left(\frac{2J_2 z_2}{N}\right)^2 \gamma_{2+3}\gamma_{5+6} u_1 v_2 u_3 u_4 v_5 u_6 \times \sum_{\vec{q}} \frac{u_{\vec{q}}^2}{\hbar(\omega_{\alpha_1} + \omega_{\alpha_2} + \omega_{\beta_3} - \omega_{\alpha_q})} \times \alpha_1 \alpha_2 \beta_3 \alpha_4^\dagger \alpha_5^\dagger \beta_6^\dagger \Delta(\vec{k}) . \tag{57}$$

If we approximate the energy denominator within the sum by $2z_2 J_2 S$ then this interaction would appear to be of the order of $2J_2 z_2/NS$, the same as the six-magnon interaction in first order. However, as we noted above, the density of states favors thermal magnons with large wave vectors. This means that the wave vectors $k_2 + k_3$ and $k_5 + k_6$ will be large making γ_{2+3} and γ_{5+6} small. This makes higher-order vertex corrections of this form small. Furthermore, all the four-magnon terms which can be combined in this manner involve β modes, in the input or output, and possibly the intermediate state. Consequently, their lower occupation further reduces this contribution so that it may be neglected.

Having obtained the vertex of the interaction in closed form, we can reach a general expression for the n-magnon relaxation. We first note that in the high-temperature approximation the integral $I^{(n)}(T)$ can be written

$$I^{(n)}(T) = a_{(n)} \left(\frac{\hbar \bar{v} k_{\max}}{k_B T}\right)^{2n-6} . \tag{58}$$

Also we approximate the magnon velocity as

$$\bar{v} = \omega_{ZB}/k_{\max} , \tag{59}$$

where

$$\omega_{ZB} = \gamma(H_E^2 + H_C^2)^{1/2} \simeq \gamma H_E , \tag{60}$$

$$k_{\max} = \pi/\Omega^{1/3} . \tag{61}$$

Using these results in Eqs. (48) and (49) we obtain for the relaxation rate due to the n-magnon processes

$$\eta_1^{(n)} = \frac{\pi}{4}\omega_0 a_{(n)} b_{(n)}^2 (u_0 v_0)^2 \frac{(\pi k_B T)^{n-2}}{(4S^2 J_2 z_2)^{n-2}} . \tag{62}$$

We now recall the expression for the Néel temperature

$$T_N = \tfrac{2}{3} S(S+1) J_2 z_2 \tag{63}$$

which allows Eq. (62) to be written in terms of the temperature normalized with respect to the Néel temperature. Using the value for $u_0 v_0$ from Eq. (16) with the approximation $H_A \ll H_E$, and using Eqs. (56) and (63) in (62), we obtain

$$\eta_1^{(n)} = 2\pi\omega_0 a_{(n)} (H_E/H_C)^2 \frac{n[(n-5)!!]^2}{2^n} \left(\frac{S+1}{12S/\pi}\right)^{n-2} \times \left(\frac{T}{T_N}\right)^{n-2} . \tag{64}$$

Finally, we note that the coefficient $a_{(n)}$ from the high-temperature value of the integral $I^{(n)}$, can be written

$$a_{(n)} \simeq 1/2^{n-3} . \tag{65}$$

Thus the n-magnon relaxation rate in the high-temperature region becomes

$$\eta_1^{(n)}|_{\text{high}T} = \pi\omega_0 \left(\frac{H_E}{2H_A}\right) n[(n-5)!!]^2 \left(\frac{S+1}{48S/\pi}\right)^{n-2} \times \left(\frac{T}{T_N}\right)^{n-2} . \tag{66}$$

E. Other relaxation mechanisms

A priori one cannot identify the dominant relaxation mechanism. This can only be determined by exploring various possibilities. The point of this paper is that in all the antiferromagnets we have analyzed the relaxation for $T < T_N$ is governed by magnon-magnon processes. We have, however, considered various other possibilities. In this section we shall review some of these.

1. Magnon-phonon

The magnon-phonon interaction arises from the phonon modulation of the exchange (exchange striction) and anisotropy (magnetostriction). The latter is generally larger and takes the form

$$\mathcal{H}_{\text{mag-ph}} = \sum_i b_{\alpha\beta\gamma\delta} S_i^\alpha S_i^\beta \frac{\partial u_i^\gamma}{\partial x^\delta} , \tag{67}$$

where u_i^γ is the displacement of the ith ion in the γ direction. This is just an expansion of the anisotropy energy in powers of the strain. By considering only the first term we are restricting ourselves to one-phonon processes. In particular, the strain is related to phonon amplitudes $c_{\vec{q}\mu}$ by

$$\frac{\partial u_i^x}{\partial y} = \sum_{\vec{q},\mu} \left(\frac{\hbar}{2\rho v \omega_{q\mu}}\right)^{1/2} (\hat{\epsilon}_\mu \cdot \hat{x})\, q_y \times (c_{\vec{q}\mu} e^{i\vec{q}\cdot\vec{R}_i} - c_{\vec{q}\mu}^\dagger e^{-i\vec{q}\cdot\vec{R}_i}), \tag{68}$$

where $\hat{\epsilon}_\mu$ is the polarization vector associated with the μth mode.

In the presence of inversion symmetry the interaction (67) reduces to

$$\mathcal{H}_{\text{mag-ph}} = b_1 \sum_{l=i,j} \left[(S_l^x)^2 \frac{\partial u_x}{\partial x} + (S_l^y)^2 \frac{\partial u_y}{\partial y} + (S_l^z)^2 \frac{\partial u_z}{\partial z}\right] + b_2 \sum_{l=i,j} (S_l^x S_l^y + S_l^y S_l^x)\left(\frac{\partial u_x}{\partial y} + \frac{\partial u_y}{\partial x}\right) + \text{permutations} . \tag{69}$$

Among the "permutation" terms are those involving $S_l^x S_l^z$. When these operators are expanded in magnon amplitudes they give one- and three-magnon terms multiplying the one-phonon amplitude. The one-phonon–one-magnon terms hybridize the magnons and phonons giving rise to the coupled modes observed, for example, in FeF_2 by inelastic neutron scattering.[26] Such experiments provide a direct measure of the interaction constant b_2. The three-magnon–one-phonon terms constitute a relaxation channel as do the four-magnon–one-magnon terms arising from the contributions to Eq. (69) involving $S_l^x S_l^y$, S_l^{x2}, etc. As in the four-magnon case those magnons near the Brillouin zone boundary will be most effective in relaxing the $\vec{k}=0$ mode. The dominant contributions to the *four-magnon–one-phonon* interaction are therefore

$$\mathcal{H} = \frac{3b_2}{2N} \sum_{k_1 k_2} \sum_{k_3 k_4} \sum_{q\mu} \left(\frac{\hbar}{2\rho v \omega_{q\mu}}\right)^{1/2} [(\hat{\epsilon}_\mu \cdot \hat{x})\, q_y + (\hat{\epsilon}_\mu \cdot \hat{y})\, q_x] \times (c_{q\mu} + c_{-q\mu}^\dagger)\,[u_1 u_2 v_3 u_4 \alpha_1 \alpha_2 \beta_3^\dagger \alpha_4^\dagger \Delta(\vec{k}) + u_1 u_2 v_3 u_4 \beta_1^\dagger \beta_2^\dagger \alpha_3 \beta_4 \Delta(\vec{k}) + \text{H.c.}] . \tag{70}$$

This involves three distinct mechanisms for relaxing the $\vec{k}=0$ mode depending upon the other input and output particles. It can be shown that the contributions proportional to b_1 are much smaller, assuming b_1 itself is not appreciably larger than b_2.

The calculation proceeds just as in the magnon case. The phonon polarizations slightly complicate the angular integrations. Let us define $\vec{q} = q(\sin\theta\cos\phi, \sin\theta\sin\phi, \cos\theta)$ and choose one transverse phonon polarized in the xy plane,

$$\hat{\epsilon}_1 = (\sin\phi, -\cos\phi, 0) . \tag{71}$$

The other polarization then becomes

$$\hat{\epsilon}_2 = \hat{\epsilon}_1 x \frac{\vec{q}}{q} = (-\cos\theta\cos\phi, -\cos\theta\sin\phi, \sin\theta) . \tag{72}$$

Following the same procedure used to calculate the four-magnon relaxation rate with the additional approximations that all the wave vectors are collinear and that the phonon group velocity equals that of the magnons (this gives optimum coupling) we obtain

$$\eta_1^{(4\text{mag}-1\text{ph})} = \frac{36\pi b_2^2}{\hbar\rho v^2} \frac{64\pi^3}{5(2\pi)^9} \Omega^2 v_0^2 \int dk_4 k_4^2 \int dq\, q^2 \int dk_3 k_3^2 e^{\hbar(\omega_2+\omega_q)/k_B T} (e^{\hbar\omega_1/k_B T} - 1)\, \bar{n}_2 \bar{n}_3 \bar{n}_4 \bar{n}_q \frac{k_3 + k_4 - k_q}{k_3 + k_4} , \tag{73}$$

where $k_2 = k_3 + k_4 - q$.

We have also carried out the calculation for the *three-magnon–one-phonon* process. Although this involves one less particle its contribution is an order of magnitude smaller than that given by Eq. (73) due to restrictions imposed by energy and momentum conservation.

2. *Magnon-exciton*

The optical spectra of many antiferromagnets show narrow, weak, magnetic dipole transitions. These are associated with pure electronic transitions within the ground-state multiplet configuration and correspond to Frenkel excitons with $\vec{k}=0$. The linewidth of these excitons is due to magnon scattering. This suggests that we consider the contribution to the magnon linewidth arising from exciton scattering in those cases where low-lying excitons exist.

FeF_2 is a likely candidate for this mechanism. The Fe^{2+} ion has a ^5D ground state. In the rutile structure this splits as shown in Fig. 4. Kambara[27] has estimated that the orthohombic crystal-field splittings are much larger than the spin-orbit and

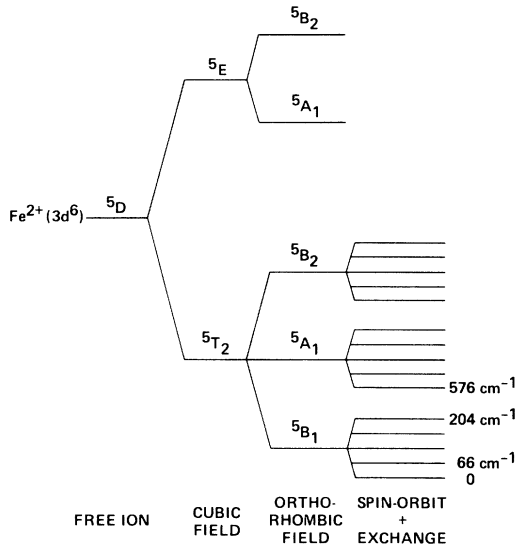

FIG. 4. Lowest-lying electronic states in FeF_2 (after Ref. 27).

exchange effects. Therefore, the excitons will not intersect the magnon dispersion curve.

Physically, the magnon-exciton interaction arises from the fact that when an ion is excited to some higher-lying spin multiplet both the spin of this state S' and its exchange coupling to its neighboring spins J' may differ from the ground-state values. Thus, in the presence of an exciton, a magnon effectively sees an impurity from which it scatters. This interaction takes the form

$$\mathcal{H}_{\text{ex-mag}} = \sum_{i,\delta} (J'\vec{S}'_i \cdot \vec{S}_{i+\delta} - J\vec{S}_i \cdot \vec{S}_{i+\delta})\, d_i^\dagger d_i \ , \qquad (74)$$

where $d_i^\dagger$ creates an excited state at site i. The ground-state spin operators have the representation given in Eq. (10). We shall express the excited-state spin by expressions of the form[28]

$$S_i'^{+} = \sqrt{2S'}\, a_i \ .$$

Note that we use the same boson operators for these excited-state spin deviations. The interaction Eq. (74) then takes the form of a *two-magnon–two-exciton* process. The relaxation calculation is then mathematically identical to the four-magnon calculation. However, in antiferromagnets the excitons have very small dispersion because nearest-neighbor transfers are spin forbidden. Consequently, if the $\vec{k} = 0$ mode scatters with a thermal exciton, and if the output exciton has the same energy then the output magnon must have $\vec{k} = 0$, which is to say that this is not a viable relaxation mechanism.

III. APPLICATIONS

In this section we shall apply the relaxation theory presented in Sec. II to several uniaxial antiferromagnets for which there are available AFMR linewidth data. We have chosen materials that have simple crystallographic and magnetic structures and that are somewhat representative of different classes of antiferromagnets. The first application is MnF_2. As we noted in Sec. II many of the approximations in this theory were developed with the data on MnF_2 as a guide. $GdAlO_3$ is another widely studied antiferromagnet. Its exchange field, and consequently its Néel temperature, is an order of magnitude smaller than MnF_2. Thus it provides a test for the numerical results of the theory for a different scale of parameters. Also, perhaps more interesting, its Gd^{3+} has an S ground state with $S = \frac{7}{2}$, which being larger than in MnF_2 ($S = \frac{5}{2}$), implies that it should be even better described by spin-wave theory. FeF_2 has the same structure as MnF_2 and comparable exchange constants. However, due to the Fe^{2+} nonzero orbital angular momentum and associated spin-orbit–crystal-field couplings, it has a large magnetocrystalline anisotropy field and magnetoelastic interaction. The large anisotropy results in a large spin-wave gap which produces marked changes in the magnon-magnon scattering processes. The magnetoelastic interaction provides an additional relaxation channel through magnon-phonon scattering. Finally, Rb_2MnF_4 and K_2MnF_4 are nearly ideal two-dimensional antiferromagnets, which provide a test of how sensitive the theory is to dimensionality. Due to this variety of different aspects associated with the different materials we shall discuss them individually.

The integrals remaining in Eq. (34) are easily evaluated numerically. Such numerical evaluation also enables us to take into account several effects, such as the finite size of the Brillouin zone and the magnon energy renormalization, which become important at higher temperatures. The energy renormalization is an important feature of spin-wave theory, whose effect appears in various physical properties such as the sublattice magnetization.[29] Since this renormalization arises from the same n-magnon interaction we have been considering, one could in principle calculate $\omega_k(T)$. However, this has to be done self-consistently and even for the four-magnon interaction the calculation is not simple. In our linear magnon dispersion relation we shall represent the effect of renormalization by writing

$$\omega_k(T) = \omega_0(T) + [\omega_{k_{\max}}(T) - \omega_0(T)]\, k/k_{\max} \ , \qquad (75)$$

i.e., we assume that the renormalization is linear

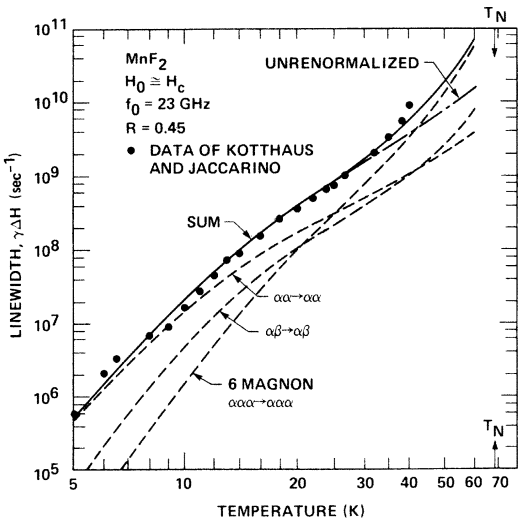

FIG. 5. Results of the four- and six-magnon calculations for MnF_2.

in k. For MnF_2 the temperature dependences of both the gap frequency and the zone-boundary energy have been measured, respectively, by AFMR techniques and neutron scattering. For the other materials we are considering there are available data for $\omega_0(T)$ but not for $\omega_{k_{max}}(T)$. Thus we have introduced an adjustable parameter

$$R = \frac{1-\omega_{k_{max}}(T)/\omega_{k_{max}}(0)}{1-\omega_0(T)/\omega_0(0)} \tag{76}$$

which is a measure of the relative renormalizations of the zone-boundary and zone-center magnons. Having $\omega_0(T)$ we can calculate $\omega_{k_{max}}(T)$ for each value of the temperature.

A. MnF_2.

The low-temperature linewidth of MnF_2 was measured in AFMR experiments at zero fields ($f_0 \simeq 260$ GHz) several years ago by Johnson and Nethercot[7] (JN). As discussed in the Introduction, the JN results at low temperatures are not applicable mainly due to radiation damping effects. The Kotthaus-Jaccarino[18] experiments avoided this problem by means of a large applied field which drives one of the magnon branches down into low-microwave frequency ranges. The KJ data, taken up to about $\frac{1}{2}T_N$ ($T_N = 68$ °K), are compared with the results of the theory in Fig. 5. The integrals of the four-magnon relaxation rates were evaluated numerically by dividing the range from $k = 0$ to $k = k_{max}$ into 50 points and using simple coarse sums. The integrals in the six-magnon rate were calculated with only 15 points, to save computer time. Some checks indicated that the results differed from the ones with 50 points by no more than 10%. The calculations were made with no additional approximations. In particular, we have used the full k-dependent coupling coefficients. For the four-magnon processes these are given by Eq. (35) and in the text below this equation. The corresponding expression for the six-magnon coefficient arising from exchange is

$$C^{(6)} = (J_2 z_2/16N^2S)\,(u_1v_2v_3v_4v_5v_6\gamma_1 + v_1v_2v_3v_4v_5u_6\gamma_6 + v_1u_2u_3u_4u_5u_6\gamma_1 + u_1u_2u_3u_4u_5v_6\gamma_6 - 2u_1v_2v_3u_4u_5v_6\gamma_{6-2-3} - 2u_1u_2v_3v_4v_5u_6\gamma_{4+5-3})\,. \tag{77}$$

The relaxation rate for the six-magnon process was obtained from Eq. (27) with Eqs. (46) and (47). For MnF_2 we used $\omega_0 = 2\pi \times 23 \times 10^9$ sec^{-1}, $H_E = 549$ kOe, and $H_A = 7.87$ kOe. The values $\omega_0(T)$ were taken from the AFMR data of JN. For R defined by Eq. (76) we used 0.45, which is an average value obtained from the neutron scattering data[30] in the high-temperature region where renormalization is important. There is one more parameter which may be considered adjustable in the applications of the theory, namely, the value of the maximum wave vector k_{max}. It determines not only the upper limits of the integrals in Eq. (34) but also the slope of the dispersion relation, Eq. (59). Therefore its value should be chosen so as to weight properly the region of the Brillouin zone that contributes most to the integral. In MnF_2, with its gap of 1 °K, the relevant magnons are those near the center of the zone, as demonstrated by the weighted magnon population shown in Fig. 2. Therefore, we use the value which correctly describes the dispersion relation at small k, which is $k_{max} = \pi/a$.[31] The total relaxation rate shown in Fig. 5 is in excellent agreement with the KJ data. At temperatures below about 25 °K, the relaxation is dominated by four-magnon intramode ($\alpha\alpha \rightarrow \alpha\alpha$) scattering, as previously found by WFW. At this temperature intermode scattering ($\alpha\beta \rightarrow \alpha\beta$) is already comparable to the intramode, which is explained by the fact that the gap of the β mode is 22 °K. Above this value the six-magnon decay rate dominates the linewidth. The reason that the six-magnon process becomes important at a relatively low temperature is due to the partial cancellation

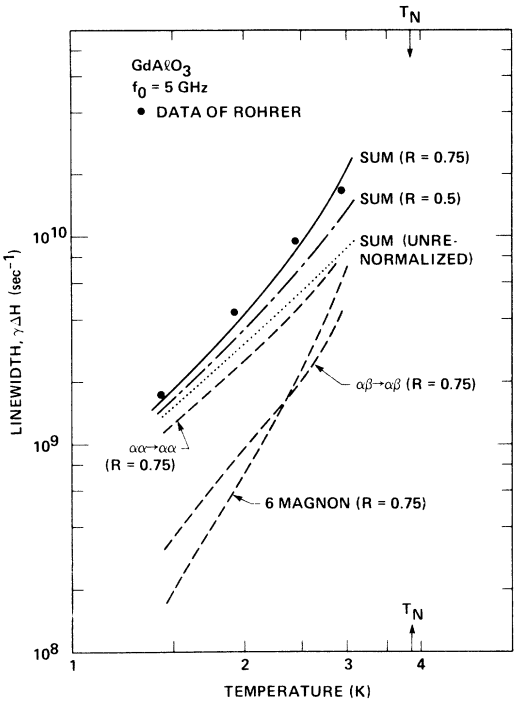

FIG. 6. Results of the four- and six-magnon calculations for $GdAlO_3$.

of the $u_0 v_0$ and v_0^2 terms in the four-magnon vertex, Eq. (38). Such interference does not occur in the six-magnon vertex or higher-order vertices as given by Eq. (54). Consequently, the higher-order process will be reduced by successively higher powers of the average magnon population $\bar{n}$ given, for example, in Fig. 2.

B. $GdAlO_3$

This material is an orthorhombic antiferromagnet with $T_N = 3.87$ °K in which the magnetic ions (Gd^{3+}) are in the S state and therefore free from strong interactions with the crystalline fields. Despite the fact that its anisotropy is orthorhombic, if the external field is applied in the bc plane it behaves essentially as an uniaxial antiferromagnet.[32] Therefore, we have calculated its AFMR linewidth due to four-magnon scattering using Eq. (34) and the analogous equation for six-magnon scattering. We used $S = 3.5$, $g = 2$, $H_E = 21$ kOe, $H_A = 3.6$ kOe, and assumed that $\omega_0(T)$ scales with $M(T)$, for which there are available data[32] (this is a very good approximation at higher temperatures). The AFMR linewidth for this material has been measured by Rohrer,[33] with standard magnetic resonance techniques and by Doussineau and Ferry,[34] using acoustic absorption. Since they are in reasonable agreement, we compare our results with those of Rohrer, who has also measured the frequency dependence of ΔH. Figure 6 shows the results of the calculations for $f_0 = 5$ GHz. Here we have used $k_{max} = (6\pi^2/\Omega)^{1/3}$, which is the proper value of k_{max} that gives the total number of magnons in the Brillouin zone equal to N. The reason for this choice is that the $k = 0$ magnons have an energy which is nearly half the zone-boundary energy. Therefore the density of states peaks sharply around the zone-boundary energy and one cannot use the small-k approximation; otherwise the missing states close to the zone edge result in gross underestimates of the linewidth. These observations have also been made in connection with other calculations[31] and are also applicable to the FeF_2 case considered next. Figure 6 shows that the calculations done with $R = 0.75$ are in very good agreement with Rohrer's data. Notice that the six-magnon decay rate does not overcome the four-magnon rate, in this case, due to the fact that the low thermal population of the zone-boundary magnons favors the latter. In Fig. 7 we also compare our results with the linewidth data as a function of frequency. Note that at low frequencies the energy gap can be neglected in the magnon populations which enter in Eq. (34), so that the frequency dependence of the relaxation rate is contained solely in the term $(e^{\beta\omega_1} - 1)$. Thus in this region the decay rate varies linearly with the frequency, as seen in Fig. 7. At larger frequencies the magnon population tends to decrease and the decay rate becomes nearly independent of the frequency.

C. FeF_2

The inelastic neutron scattering experiments by Rainford *et al.*[26] clearly show that the phonons couple strongly to the magnons in FeF_2 an effect which, incidently, cannot be detected in MnF_2. The coupling constant b_2 derived from these measurements is of the order of 10^{-15} erg. As we

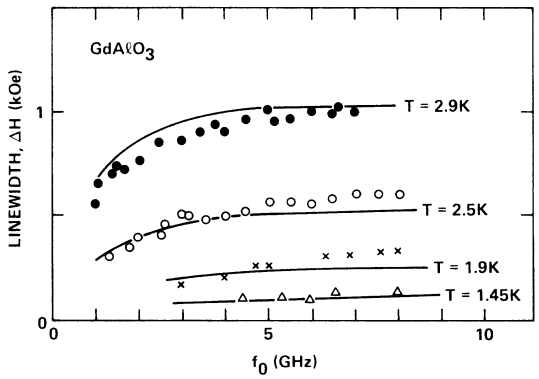

FIG. 7. Comparison of the theoretical (lines) and experimental (points from Ref. 33) frequency dependence of the linewidth in $GdAlO_3$.

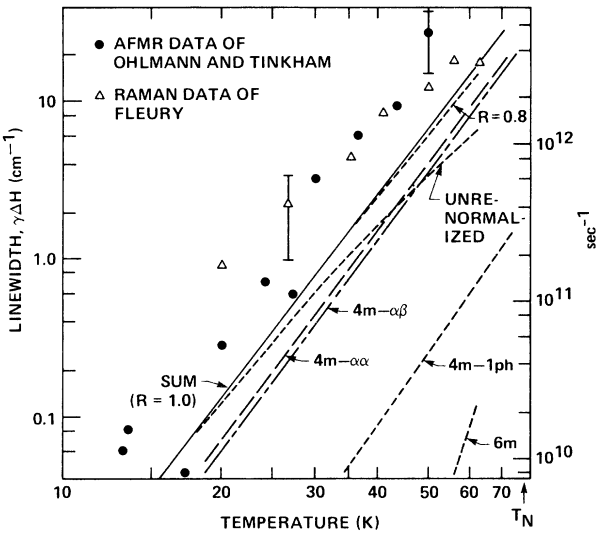

FIG. 8. Comparison of various relaxation processes with experimental data for FeF_2. The dashed lines were all computed with $R=1$.

saw in Sec. II E 1 the strongest magnon-phonon mechanism is the four-magnon–one-phonon process. The measured value of b_2 makes the ratio of the four-magnon–one-phonon vertex to the four-magnon vertex only of order $\frac{1}{10}$. The relaxation rate given by Eq. (72) is shown in Fig. (8). Parameters used in the calculations are $S=2$, $g=2.2$, $H_A=200$ kOe, and $H_E=580$ kOe. We see that this contribution cannot account for the measured,[8,35] linewidths.

The decay rates from the magnon-magnon interactions were evaluated as in the previous cases and are also shown in Fig. 8. As in the $GdAlO_3$ case we have chosen $k_{max}=(6\pi^2/\Omega)^{1/3}$ because the weighted magnon population over the entire temperature range of interest is largest at the edge of the Brillouin zone as shown in Fig. 9.

The results of the calculations are in satisfactory agreement with the experimental data, if one considers the approximations used and the fact that the experimental errors (the vertical bands in the figure indicate the instrumental width) are quite significant at lower temperatures, because the zero-temperature linewidth was subtracted from the measured values. We note that the relaxation is entirely dominated by four-magnon processes of the two types. The higher-order processes give negligible contribution as in the $GdAlO_3$ case because the magnon population is small due to the large energy gap (compare the populations in Fig. 9 with those for MnF_2, in Fig. 2).

D. Two-dimensional antiferromagnets

The isomorphic compounds Rb_2MnF_4, K_2MnF_4, and K_2NiF_4 behave as almost ideal two-dimensional (2D) antiferromagnets, due to the very weak exchange interaction between the spins in planes perpendicular to the c axis. Their magnetic properties were extensively investigated by Breed *et al.*[36] and the AFMR linewidths of the first two compounds were recently measured by de Wijn *et al.*[37] The linewidth data are shown in Fig. 11. It is interesting to note that in this lower dimension the linewidth also has a T^4 dependence as one finds in several of the 3D systems.

The two-dimensional aspect, however, presents distinct differences. When the sums over wave vector are replaced by integrals the integration over k_z is trivial since the magnon energies are independent of k_z. This leaves us with two dimensional integrals of the form $\int k\,dk\,d\phi$. The fact that we integrate over ϕ and not $\cos\phi$ introduces an important difference. In the four-magnon process, for example, the energy conserving δ function is given in Eq. (33). Since $\delta(\cos\theta_{23}-1)=\delta(\theta_{23})/\sin\theta_{23}$ the integral over θ_{23} gives zero since $\delta(\theta)$ is an even function of θ while $\sin\theta$ is odd. This is a consequence of the fact that in two dimensions energy and momentum restrict the phase space to one point. Equation (47) shows that a similar restriction occurs in all the higher-order processes if we make the "collinear" approximation. However, due to the presence of k, rather than k^2 in the integrals, small-k magnons

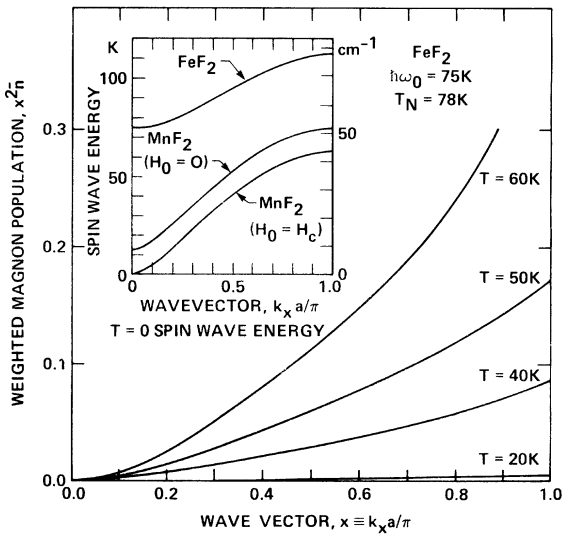

FIG. 9. Weighted magnon population curves as a function of wave vector for FeF_2 in zero applied field. Insert contrasts the spin-wave dispersion relation of FeF_2 with that of MnF_2.

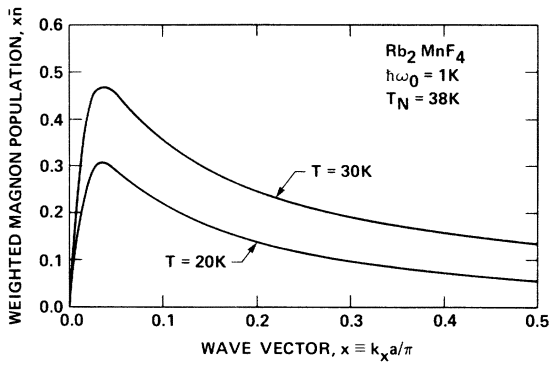

FIG. 10. Weighted magnon population curves as a function of wave vector for the two-dimensional antiferromagnet Rb_2MnF_4.

play a much more important role here than in 3D systems. This is clearly seen in the plots of the weighted magnon population shown in Fig. 10. In this low-k region the magnon dispersion relation deviates from a true linear relation due to the presence of the gap. We shall therefore use a quadratic relation of the form $\omega_k = \omega_1 + Dk^2$. Another consequence of the reduced dimensionality is that the high-temperature approximation $\beta\hbar\omega_k \ll 1$ is very good for temperatures larger than the energy gap, which in the case of the experiments we shall consider is only 1 °K. This offers the hope for obtaining a completely analytical result for the linewidth.

With the quadratic dispersion relation one can treat energy and momentum conservation exactly in the four-magnon processes in which $k_1 = 0$ and $\delta(\omega) = (2Dk_3k_4)^{-1}\delta(\cos\phi_{34})$, where ϕ_{34} is the angle between $\vec{k}_3$ and $\vec{k}_4$. In this case $\vec{k}_3$ and $\vec{k}_4$ must be at *right angles* to each other, rather than collinear. Elliminating the integral in k_2, the decay rate for the k_1 magnon due to four-magnon processes can be written

$$\eta_1^{(4m)} = (e^{\beta\hbar\omega_1} - 1)\frac{a^4}{4\pi^2\hbar^2 D} \times \int dk_3 \int dk_4 |NC^{(4)}|^2 e^{\beta\hbar\omega_2}\bar{n}_{3+4}\bar{n}_3\bar{n}_4 , \tag{78}$$

where the coupling coefficients are the same as given in Eq. (34).

The numerical calculations for Rb_2MnF_4 and K_2MnF_4 show that the four-magnon relaxation rate has a smaller T dependence than the measured T^4 and is nearly an order of magnitude smaller. We therefore consider the six-magnon process. There are two reasons why we might expect this process to be more important. First, since small-k states dominate the integrations, the coupling coefficient for four-magnon processes is approximately $C^{(4)}(0,0,0,0)$, which involves factors of the type $(u_0 - v_0)^2$. This greatly reduces the exchange four-magnon coupling. Due to the effect of anisotropy this is slightly enchanced in the $\alpha\beta$ scattering but reduced even further in the $\alpha\alpha$ scattering. In the six-magnon coupling coefficient all the contributions add constructively to enlarge them relative to the four-magnon coefficient as we pointed out for MnF_2. In addition to this, in 2D systems the addition of more particles in the scattering process does not reduce the decay rate as much as in 3D because the occupation number is relatively large. This is so both because the energy of the dominating low-k magnons is small and because the energy of all magnons with $\vec{k}//\hat{c}$ have the same small gap.

Let us now consider the six-magnon process in detail. The relaxation rate is obtained in a manner analogous to the 3D case. As in that case the conservation of energy and momentum results in a complicated coupling between the wave vector sums. The energy δ function is

$$\delta(\omega) = (1/D)\delta(k_2^2 + k_3^2 - k_4^2 - k_5^2 - k_6^2) . \tag{79}$$

In the 3D, four-magnon case we found that energy and momentum conservation required that all the wave vectors be collinear. We therefore extended this condition to the six-magnon case. In the 2D four-magnon case we have just seen that the two output wave vectors must be orthogonal. Therefore, let us introduce the relative wave vector $\vec{k} = \vec{k}_2 - \vec{k}_6$ and require that $\vec{k} \perp \vec{k}_3$ and $\vec{k}_4 \perp \vec{k}_5$. The energy δ function then reduces to

$$\delta(\omega) \to (1/2Dkk_6)\delta(\theta_6 - \tfrac{1}{2}\pi) , \tag{80}$$

where θ_6 is the angle $\vec{k}_6$ makes relative to $\vec{k}$. Since momentum conservation requires $\vec{k} = \vec{k}_4 + \vec{k}_5 - \vec{k}_3$, the sum on $\vec{k}_2$ (or, equivalently, $\vec{k}$) may be performed. If we assume that the coupling coefficient is independent of wave vector and make the high-temperature approximation the relaxation rate becomes

$$\eta_1^{(6m)} = \frac{\omega_1 a^8}{2^5\pi^4\hbar^2 D} N^2 |C^{(6m)}|^2 \left(\frac{k_B T}{\hbar}\right)^4 I , \tag{81}$$

where

$$I = \int_0^{k_{\max}} \frac{k_3 dk_3}{\omega_1 + Dk_3^2} \int_0^{k_{\max}} \frac{k_4 dk_4}{\omega_1 + Dk_4^2} \int_0^{k_{\max}} \frac{k_5 dk_5}{\omega_1 + Dk_5^2} \int_0^{k_{\max}} \frac{dk_6}{(\omega_1 + Dk_6^2)(k_4^2 + k_5^2 - k_3^2)^{1/2}(\omega_1 + Dk_1^2 + Dk_5^2 - Dk_3^2 + Dk_6^2)} . \tag{82}$$

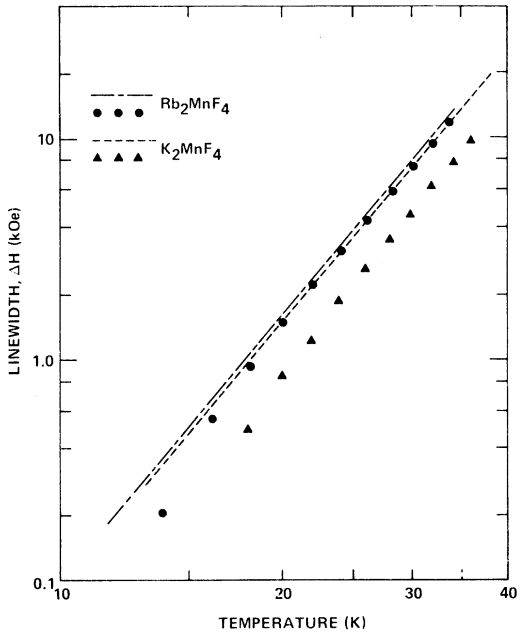

FIG. 11. Comparison of the six-magnon calculation for the two-dimensional antiferromagnets Rb_2MnF4 and K_2MnF_4, with the experimental results.

Estimating this integral we obtain

$$I \simeq \pi^2/4\omega_1^2 D^3 . \tag{83}$$

For the coupling coefficient we use the approximate form

$$|C^{(6)}|^2 = (4J^2/12N^4S^2)(u_0^2 v_0^2)^2 . \tag{84}$$

The relaxation rate therefore becomes

$$\eta_1^{6m} \sim [(k_B T)^4/384\hbar^4 S^4 (\gamma H_c)^2 \omega_1] . \tag{85}$$

This is plotted as the dashed lines in Fig. 11. The crudeness of our approximations have suppressed the differences between the two compounds. However, we see that the six-magnon process gives the correct order of magnitude and temperature dependence.

IV. CONCLUSION

In this paper we have demonstrated that the temperature dependence of the magnetic resonance linewidth in antiferromagnets arises primarily from spin-wave scattering processes. In particular, we have investigated magnon-phonon and magnon-exciton processes in several antiferromagnets and find that these are not effective relaxation channels. Presumably if one has a material consisting of non-S state magnetic ions and having a very low Néel temperature the magnon-phonon mechansim could become important.

Another interesting result of our investigation is that in a number of situations, particularly the two-dimensional antiferromagnets, the lowest order spin-wave process that dominates the relaxation at $T > \frac{1}{4} T_N$ involves *six* magnons. The fact that one must go to this order in spin-wave theory makes one also question its role in describing other thermodynamic properties of antiferromagnets. The general theory developed in Sec. II works surprisingly well for all the materials considered over a relatively wide range of temperatures up to $0.8\, T_N$, a conclusion which is also supported by the calculation of other quantities based on spin-wave theory.

The authors would like to acknowledge helpful contributions from Professor L. C. M. Miranda, Professor B. Zeks, and E. F. Sarmento at different stages of this work.

*Supported by a fellowship of the J. S. Guggenheim Memorial Foundation.

†Work supported by Banco Nacional de Desenvolvimento Economico (BNDE), Conselho Nacional de Desenvolvimento Cientifico e Tecnológico (CNPq) and CAPES (Brazilian Government) and the National Science Foundation.

[1]T. Holstein and H. Primakoff, Phys. Rev. 58, 1098 (1940).

[2]See, for example, A. I. Akhiezer, V. G. Baryakhtar, and S. V. Peletminskii, *Spin Waves* (North-Holland, Amsterdam, 1968), Chap. 8.

[3]S. V. Maleev, Zh. Eksp. Teor. Fiz. 33, 1010 (1957) [Sov. Phys.-JETP 6, 776 (1958)].

[4]F. J. Dyson, Phys. Rev. 102, 1217 (1956); 102, 1230 (1956).

[5]T. Oguchi, Prog. Theor. Phys. 25, 721 (1961); Phys. Rev. 117, 117 (1960).

[6]J. I. Davis, Ann. Phys. 58, 529 (1970).

[7]F. M. Johnson and A. H. Nethercot, Jr., Phys. Rev. 114, 705 (1959).

[8]R. C. Ohlmann and M. Tinkham, Phys. Rev. 123, 425 (1961).

[9]R. Loudon and P. Pincus, Phys. Rev. 132, 473 (1963).

[10]U. N. Upadhyaya and K. P. Sinha, Phys. Rev. 130, 939 (1963).

[11]V. N. Genkin and V. M. Fain, Zh. Eskp. Teor. Fiz. 41, 1522 (1961) [Sov. Phys.-JETP 14, 1086 (1962)].

[12]K. Tani, Prog. Theor. Phys. 30, 580 (1963); 31, 335 (1964).

[13]P. Pincus, J. Phys. Radium 23, 536 (1962).

[14]J. Solyom, Zh. Eksp. Teor. Fiz. 55, 2355 (1968) [Sov. Phys.-JETP 28, 1251 (1969)].

[15]M. I. Kaganov, V. M. Tsukernik, and I. Y. Chupis, Fiz. Metal. Metaloved. 10, 797 (1960) [Phys. Metal. Metallogr. 10, 154 (1960)].

[16]M. G. Cottam and R. B. Stinchcombe, J. Phys. C 3, 2326 (1970).

[17]A. B. Harris, D. Kumar, B. I. Halperin, and P. C. Hohenberg, Phys. Rev. B 3, 961 (1971).
[18]J. P. Kotthaus and V. Jaccarino, Phys. Rev. Lett. 28, 1649 (1972); AIP Conf. Proc. 10, 57 (1973).
[19]S. M. Rezende, E. A. Soares, and V. Jaccarino, AIP Conf. Proc. 18, 1083 (1974).
[20]R. W. Sanders, D. Paquett, V. Jaccarino and S. M. Rezende, Phys. Rev. B 10, 132 (1974).
[21]R. M. White, R. Freedman, and R. B. Woolsey, Phys. Rev. B 10, 1039 (1974).
[22]R. M. White, S. M. Rezende, and L. C. M. Miranda, AIP Conf. Proc. 24, 172 (1975).
[23]See, for example, R. M. White, M. Sparks, and I. Ortenburger, Phys. Rev. 139, A450 (1965).
[24]See, for example, M. Sparks, *Ferromagnetic Relaxation Theory* (McGraw-Hill, New York, 1964).
[25]M. Sparks and L. J. Sham, Phys. Rev. B 8, 3037 (1973).
[26]B. D. Rainford, J. G. Houmann, and H. J. Guggenheim, in *Proceedings of the Symposium on Inelastic Scattering of Neutrons in Solids and Liquids* (IAEA, Vienna, 1972), p. 655.
[27]T. Kambara, J. Phys. Soc. Jpn. 24, 1242 (1968).
[28]J. B. Parkinson and R. Loudon, J. Phys. C 1, 1568 (1968).
[29]G. G. Low, Proc. Phys. Soc. Lond. 82, 992 (1963).
[30]G. G. Low, in *Proceedings of the Symposium on Inelastic Scattering of Neutrons in Solids and Liquids, 1964* (IAEA, Vienna, 1965).
[31]D. Paquette, A. R. King, and V. Jaccarino, Phys. Rev. B 11, 1193 (1975).
[32]J. D. Cashion, A. H. Cooke, T. L. Thorp, and M. R. Wells, Proc. R. Soc. A 318, 473 (1970).
[33]H. Rohrer, AIP Conf. Proc. 24, 268 (1975).
[34]P. Doussineau and B. Ferry, Phys. Lett. 46A, 135 (1973).
[35]P. A. Fleury, in *Proceedings of the Second International Conference on Light Scattering*, edited by M. Balkanski (Flamarion, Paris, 1971), p. 151.
[36]D. J. Breed, Physica (Utr.) 37, 35 (1967).
[37]H. W. de Wijn, L. R. Walker, S. Geschwind, and H.J. Guggenheim, Phys. Rev. B 8, 299 (1973).